



OPEN ACCESS

EDITED BY Alberto Zullo. University of Sannio, Italy

REVIEWED BY Peter R. Corridon, Khalifa University, United Arab Emirates Chunhui Li. University of Dundee, United Kingdom

*CORRESPONDENCE Quan Liu, Pengxia Wan.

[†]These authors have contributed equally to this work and share first authorship

RECEIVED 28 August 2025 REVISED 10 October 2025 ACCEPTED 31 October 2025 PUBLISHED 11 November 2025

Yang X, Ren Q, Kong X, Su P, Liu C, Liu Q and Wan P (2025) Corneal viscoelasticity is associated with intraocular pressure under physiological baseline: insights from the rheological properties of corneal lenticules. Front. Bioeng. Biotechnol. 13:1694568. doi: 10.3389/fbioe.2025.1694568

COPYRIGHT

© 2025 Yang, Ren, Kong, Su, Liu, Liu and Wan. This is an open-access article distributed under the terms of the Creative Commons Attribution License (CC BY). The use, distribution or reproduction in other forums is permitted. provided the original author(s) and the copyright owner(s) are credited and that the original publication in this journal is cited, in accordance with accepted academic practice. No use, distribution or reproduction is permitted which does not comply with these

Corneal viscoelasticity is associated with intraocular pressure under physiological baseline: insights from the rheological properties of corneal lenticules

Xiaonan Yang^{1,2†}, Qi Ren^{1†}, Xiangbin Kong², Peng Su², Chang Liu³, Quan Liu^{3,4}* and Pengxia Wan¹*

¹Department of Ophthalmology, The First Affiliated Hospital, Sun Yat-sen University, Guangzhou, China, ²Department of Ophthalmology, The Second People's Hospital of Foshan, Foshan, China, ³State Key Laboratory of Ophthalmology, Zhongshan Ophthalmic Center, Sun Yat-sen University, Guangdong Provincial Key Laboratory of Ophthalmology and Vision Science, Guangdong Provincial Clinical Research Center for Ocular Diseases, Guangzhou, Guangdong, China, ⁴Bright Eye Hospital Group, Guangzhou, China

This study aims to investigate the modulation effect of baseline intraocular pressure (IOP) on corneal viscoelastic modulus within physiological ranges. We collected 48 stromal lenticules from 26 healthy myopic patients undergoing SMILE surgery. Based on biomechanically corrected IOP (bIOP), stratifying the samples into a low-pressure group (bIOP <15 mmHg, n = 15) and a high-pressure group (bIOP ≥15 mmHg, n = 33) according to pre-operative measurements. Each fresh lenticule underwent strain-controlled torsional rheometry at 37 $^{\circ}$ C (shear strain 1%, angular frequency 0.1–100 rad s⁻¹), recording storage modulus (G'), loss modulus (G''), complex viscosity (η^*), and loss factor (tan δ), with elastic modulus (E) calculated from G'. In parallel, in vivo corneal deformation and stiffness parameters were obtained using the Corvis ST. The results showed that viscoelastic parameters increased monotonically with frequency, demonstrating solid-like behavior; in the frequency range of $10^{\circ}-10^{1.5}$ rad s⁻¹, G' and E were significantly higher in the high-pressure group compared to the low-pressure group (both p < 0.05), while the log-modulus versus log-frequency slopes showed no significant difference, indicating an upward "stiffness offset" due to elevated bIOP without altering dispersive characteristics. Corvis ST also confirmed that the high-pressure group exhibited smaller deformation amplitudes and higher stiffness parameters. Overall, even within the normal range, elevated baseline IOP results in an upward shift in corneal E without affecting its time-dependent properties, suggesting that corneal stromal rigidity is adaptable to the ocular pressure environment under physiological conditions.

corneal biomechanics, viscoelasticity, intraocular pressure, small incision lenticule extraction (SMILE), CorVis ST, torsional shear rheometry

1 Introduction

The cornea is the eye's primary refractive element and a frontline protective barrier, so its biomechanics are crucial for maintaining normal vision (Meek et al., 2025). Under physiological intraocular pressure (IOP), the cornea undergoes only minute deformations, with strains typically below 1%, within which it behaves as an essentially linear viscoelastic solid (Pang, 2021). That response is governed by the architecture of the collagen fiber network, the composition of the stromal matrix, and tissue hydration. Even within the physiological pressure range, individual corneas can respond quite differently (Vinciguerra et al., 2020; Xu et al., 2021; Liu et al., 2023; Wei et al., 2023). Quantifying corneal viscoelasticity under physiological IOP is therefore fundamental to understanding structure–function coupling and disease mechanisms in disorders such as glaucoma and keratoconus.

In vivo, the Corvis ST uses a calibrated air puff and ultra-highspeed Scheimpflug imaging to capture dynamic corneal deformation. It yields pressure-independent indices such as biomechanically corrected IOP (bIOP) and device-derived metrics including stiffness parameter at first applanation (SPA1), stiffness parameter at highest concavity (SPHC), Ambrósio's Relational Thickness in the horizontal direction (ARTh), Corvis Biomechanical Index (CBI), and the stress-strain index (SSI), among others (Renato et al., 2013; Roberts, 2014; Vinciguerra et al., 2016; Roberts et al., 2017; Eliasy et al., 2019; Vinciguerra et al., 2021; Zhang et al., 2021; Flockerzi et al., 2022; Miao et al., 2024). In addition, several derived parameters leverage dynamic corneal response (DCR) metrics to link biomechanics-related ocular diseases such as glaucoma-for example, the Biomechanical Glaucoma Factor (BGF) (Pillunat et al., 2019). These parameters reflect the cornea's resistance to transient loading, complementing ex vivo material measurements by sampling the tissue's performance at the organ scale under physiological conditions. Moreover, small incision lenticule extraction (SMILE) offers an opportunity to probe corneal stromal mechanics in humans. In SMILE, a femtosecond laser creates an intrastromal lenticule that is manually dissected and extracted through a small incision to correct myopia. The retrieved stromal lenticule preserves native extracellular matrix and collagen lamellae at physiologic hydration if handled promptly, enabling high-fidelity, ex vivo rheological testing under controlled conditions.

Quantifying corneal viscoelasticity has been approached using a range of complementary methods. Conventional rheological techniques include stress-controlled and strain-controlled oscillatory tests and steady-shear measurements. Meanwhile, strain-controlled frequency sweeps at small strains are particularly suitable for delicate collagenous tissues because they minimize structural damage while mapping storage modulus (G'), loss modulus (G''), complex viscosity (η^*), and loss factor ($\tan \delta$) across a physiologically relevant frequency band. By limiting the applied deformation to the 0.001%–1% range, these sweeps preserve the collagen framework while probing a wide frequency band (0.1–100 rad s⁻¹) that covers the characteristic rates of fixational eye movements and spontaneous retinal venous pulsations (Kim et al., 2014; Beylergil et al., 2022).

Within this context, we examined how baseline, physiological bIOP modulates corneal viscoelasticity. We hypothesized that,

within the physiological IOP range, higher baseline pressure would be accompanied by an upward shift in both G' and G'', a trend that should be observable at the macroscopic (whole cornea) and microscopic (stromal layer) scales alike. We tested this by performing small-strain, strain-controlled torsional-shear frequency sweeps on fresh stromal lenticules obtained during SMILE and, in parallel, by characterizing *in vivo* corneal deformation with the Corvis ST. Establishing a quantitative link between physiological bIOP and viscoelastic modulus may refine constitutive models and inform personalized risk stratification in glaucoma, keratoconus, and pressure-related ocular disorders.

2 Methods

This study was approved by the Ethics Committee of the Zhongshan Ophthalmic Center (2013MEKY036) and was conducted in accordance with the Declaration of Helsinki. Written informed consent was obtained from all participants before enrollment, permitting the use of their clinical data for research.

Before surgery, each subject underwent a comprehensive ophthalmic evaluation that included slit-lamp biomicroscopy, non-contact tonometry, and anterior-segment tomography. Exclusion criteria were: 1) keratoconus or suspected keratoconus; 2) IOP <10, or >21 mmHg, normal-tension glaucoma (NTG) or suspected NTG; 3) active ocular or systemic disease; 4) prior ocular trauma or surgery; and 5) any other condition known to influence corneal biomechanics.

2.1 In vivo data

In vivo corneal biomechanics were assessed with the Corvis ST (Oculus, Wetzlar, Germany; software version 1.6r2187) preoperatively and 1 day post-operatively. Only measurements labelled "OK" in the quality-specification (QS) window were included in the analysis.

2.2 Ex vivo data

SMILE was performed by a single experienced surgeon using a VisuMax femtosecond laser system (Carl Zeiss Meditec AG, Jena, Germany). After creation and manual dissection, each stromal lenticule was removed through a small incision and immediately immersed in sterile BSS Sterile Irrigating Solution (Alcon Laboratories, Inc., Fort Worth, TX, USA) at 4 °C to maintain tissue hydration.

Ex vivo rheological properties of the lenticules were measured on a DHR-2 rheometer (TA Instruments, USA) using a 20 mm parallel-plate geometry with a 0.9 mm gap. To prevent slippage and ensure no-slip boundary conditions, 320 grit sandpaper was glued to both loading platens (Hatami-Marbini, 2014). Prior to testing, specimens were equilibrated in BSS solution at 37 °C for 30 min. The submersion chamber of the rheometer was filled with BSS solution to maintain tissue hydration throughout measurements. Oscillatory frequency sweeps were performed at 37 °C with 1% strain

TABLE 1 Rheological testing parameters.

Parameter	Specification	
Rheometer	DHR-2 (TA Instruments, USA)	
Geometry	20 mm parallel plate	
Gap	0.9 mm	
Plate surface	320 grit sandpaper	
Temperature	37 °C	
Pre-equilibration	30 min in BSS at 37 °C	
Test environment	BSS submersion chamber	
Strain amplitude	1%	
Angular frequency	0.1-100 rad s ⁻¹	
Test mode	Oscillatory frequency sweep	
Time post-extraction	<2 h	

and an angular frequency (ω) of 0.1–100 rad s⁻¹. The G', G'', η^* , and tan δ were calculated to characterize viscoelastic behavior. All biomechanical tests were completed within 2 hours of extraction to minimize tissue degradation. The detailed rheological testing parameters are summarized in Table 1.

Although the cornea is anisotropic and viscoelastic, it is commonly approximated as an isotropic, linear-elastic material under small deformations. Under this assumption the elastic modulus (*E*) was derived from the storage modulus using

$$E = 2G'(1 + \nu)$$

with a Poisson's ratio (ν) of 0.40 (Ford et al., 2011).

2.3 Statistical analysis

All statistical analyses were performed using R (version 4.5.0). A total of 48 corneal stromal lenticule specimens from 26 healthy young myopic adults were stratified into two groups based on bIOP: the low-pressure group (bIOP <15 mmHg) and the high-pressure group (bIOP \geq 15 mmHg). For normally distributed data, intergroup comparisons were conducted using independent samples t-tests; otherwise, Mann-Whitney U tests were applied. Categorical variables were analyzed using Pearson's Chi-squared tests or Fisher's exact tests when appropriate. Statistical significance was defined as p < 0.05.

3 Result

A total of 48 corneal stromal lenticule specimens from 26 young myopic adults were included in the analysis. Among them, 22 subjects contributed bilateral data and four contributed unilateral data. The lenticules were stratified into two groups according to bIOP: bIOP <15 mmHg (N = 15) and bIOP $\geq\!15$ mmHg (N = 33). The primary analysis treated each lenticule as an independent observation. A sensitivity analysis using only one randomly selected eye per subject (N = 26) yielded consistent results, suggesting that inter-eye correlation did not

substantially affect the conclusions. There were no statistically significant differences in baseline characteristics such as age, gender distribution, pre-operative central corneal thickness (CCT), BGF, and parameters related to the cap, stromal lenticule, and remaining stroma bed thickness from the SMILE procedure between the two groups (all p > 0.05; Table 2).

The viscoelastic properties of the lenticules were assessed across a range of oscillatory angular frequencies. The G', G'', η^* , and $\tan \delta$ all exhibited frequency-dependent changes in both groups (Figure 1).

Across the measured frequency range (0.1–100 rad s⁻¹), the bIOP \geq 15 mmHg group consistently showed higher mean values of G' than the bIOP <15 mmHg group, indicating increased corneal stiffness. This trend was also observed for the G'', suggesting enhanced viscous damping properties in the higher bIOP group. The differences between groups were statistically significant at ω of 10^0 – $10^{1.5}$ rad s⁻¹ and above (p < 0.05). Similarly, the η^* was elevated in the bIOP \geq 15 mmHg group compared to the lower bIOP group throughout the tested frequency range. The tan δ values, reflecting the viscoelastic balance between G' and G'', displayed no significant intergroup differences across most ω .

The elastic modulus E was calculated from the storage modulus G' using $E=2G'(1+\nu)$ with Poisson's ratio $\nu=0.4$. Across the tested ω , range $(0.1\text{--}100 \text{ rad s}^{-1}, \log_{10} \text{ scale})$, E displayed the expected frequency dependence, rising steadily toward the high- ω end in both groups (Figure 2). Eyes with bIOP ≥ 15 mmHg exhibited significantly higher mean E values than those with bIOP <15 mmHg throughout the $10^0-10^{1.5}$ rad s⁻¹ spectrum (p<0.05). The between-group separation became most conspicuous at ≥ 1 rad s⁻¹, indicating that elevated IOP is accompanied by a stiffer corneal matrix, especially under rapid, small-amplitude deformation. The curves nearly converged at the lowest ω but diverged markedly above 10 rad s⁻¹. Linear mixed-model analysis indicated comparable ω -response slopes between groups, implying similar viscoelastic dispersion but a higher overall stiffness offset in the high-bIOP eyes.

4 Discussion

This study establishes a clear association between bIOP and corneal viscoelastic behavior. Using small-strain, strain-controlled torsional shear rheometry, we quantified the frequency-dependent response of stromal lenticules harvested during SMILE in a deformation mode that closely mirrors the subtle rotational micro-strains encountered *in vivo*. This bench-scale characterization directly addresses the physiological regime where the cornea operates under 1% strains as an approximately linear viscoelastic solid.

Across the examined frequency spectrum, G', G'', and the derived E rose toward the high-frequency end, as expected for a viscoelastic solid. Eyes with higher bIOP exhibited a uniform upward shift in these moduli at every tested frequency, whereas the rate at which each modulus changed with frequency remained essentially constant across pressure groups. In practical terms, elevated bIOP increases the baseline stiffness of the corneal matrix without measurably altering the underlying time-dependent relaxation mechanisms that govern energy storage and dissipation. Clinically, this aligns with reports that corneas in normal-tension glaucoma are more deformable, whereas those in high-tension glaucoma and ocular hypertension are

TABLE 2 Demographic and clinical data of the involved eyes (48 eyes from 26 patients).

Characteristic	Overall N = 48 ¹	bIOP <15 mmHg N = 15 ¹	bIOP ≥15 mmHg N = 33¹	<i>p</i> -value ²
Gender				0.7
Female	35 (73%)	12 (80%)	23 (70%)	
Male	13 (27%)	3 (20%)	10 (30%)	
Age, year	26 (7)	25 (6)	27 (7)	0.5
Eye				0.3
OD	25 (52%)	6 (40%)	19 (58%)	
OS	23 (48%)	9 (60%)	14 (42%)	
SE, diopter	-5.07 (1.33)	-5.19 (0.90)	-5.02 (1.49)	0.7
CR, mm	43.24 (1.47)	42.70 (1.24)	43.48 (1.51)	0.1
IOP, mmHg	16.59 (2.36)	14.30 (0.84)	17.64 (2.08)	<0.001
bIOP, mmHg	15.98 (2.08)	13.76 (0.72)	16.99 (1.66)	<0.001
CCT, µm	561 (29)	567 (25)	558 (30)	0.3
ARTh	687 (181)	632 (135)	712 (195)	0.2
SPA1	107 (13)	98 (8)	111 (13)	<0.001
CBI	0.017 (0.056)	0.031 (0.087)	0.011 (0.034)	0.3
TBI	0.19 (0.31)	0.31 (0.41)	0.07 (0.13)	0.2
SSI	0.97 (0.13)	0.91 (0.10)	1.00 (0.13)	0.03
BGF	0.14 (0.10)	0.12 (0.11)	0.15 (0.10)	0.4
Cap diameter, mm	7.47 (0.18)	7.49 (0.21)	7.46 (0.16)	0.7
Cap thickness, µm				0.2
120	11 (23%)	2 (13%)	9 (27%)	
125	34 (71%)	11 (73%)	23 (70%)	
130	3 (6.3%)	2 (13%)	1 (3.0%)	
Lenticule diameter, mm	6.59 (0.18)	6.61 (0.22)	6.58 (0.16)	0.6
Lenticule overlap, mm				0.7
0	10 (21%)	4 (27%)	6 (18%)	
0.1	38 (79%)	11 (73%)	27 (82%)	
Lenticule thickness, µm	108 (24)	108 (18)	108 (26)	>0.9
Lenticule basethickness, µ	ım			
10	48 (100%)	15 (100%)	33 (100%)	

¹n (%); Mean (SD).

Abbreviation: OD, right eye (Oculus Dexter); OS, left eye (Oculus Sinister); SE, spherical equivalent; IOP, intraocular pressure; bIOP, biomechanically corrected IOP; CCT, central corneal thickness; ARTh, Ambrósio's Relational Thickness horizontal direction; SPA1, Stiffness Parameter A1; CBI, corvis biomechanical index; TBI, tomographic and biomechanical index; BGF, biomechanical glaucoma factor; SSI, Stress-Strain Index; CR, corneal curvature radius.

comparatively less deformable (Liu et al., 2023). The present work provides direct torsional-shear evidence consistent with that trend and supports the view that healthy corneas are stabilized against large deformations by stress-stiffening mechanisms (McMonnies and Boneham, 2007). A plausible structural explanation is a modest increase in collagen packing density or cross-link density that stiffens the fibrillar backbone while leaving the molecular relaxation spectrum largely intact. Whether such material changes are a cause or a

consequence of higher IOP cannot be resolved in a cross-sectional study; longitudinal designs that integrate *in vivo* imaging with *ex vivo* rheometry are warranted.

These findings also dovetail with organ-scale *in vivo* metrics obtained using the Corvis ST. Pressure-independent indices such as bIOP, together with DCR-derived parameters that link corneal biomechanics to ocular disease—for example, the BGF (Pillunat et al., 2019)—reflect resistance to transient loading under

²Fisher's exact test; One-way analysis of means; Pearson's Chi-squared test.

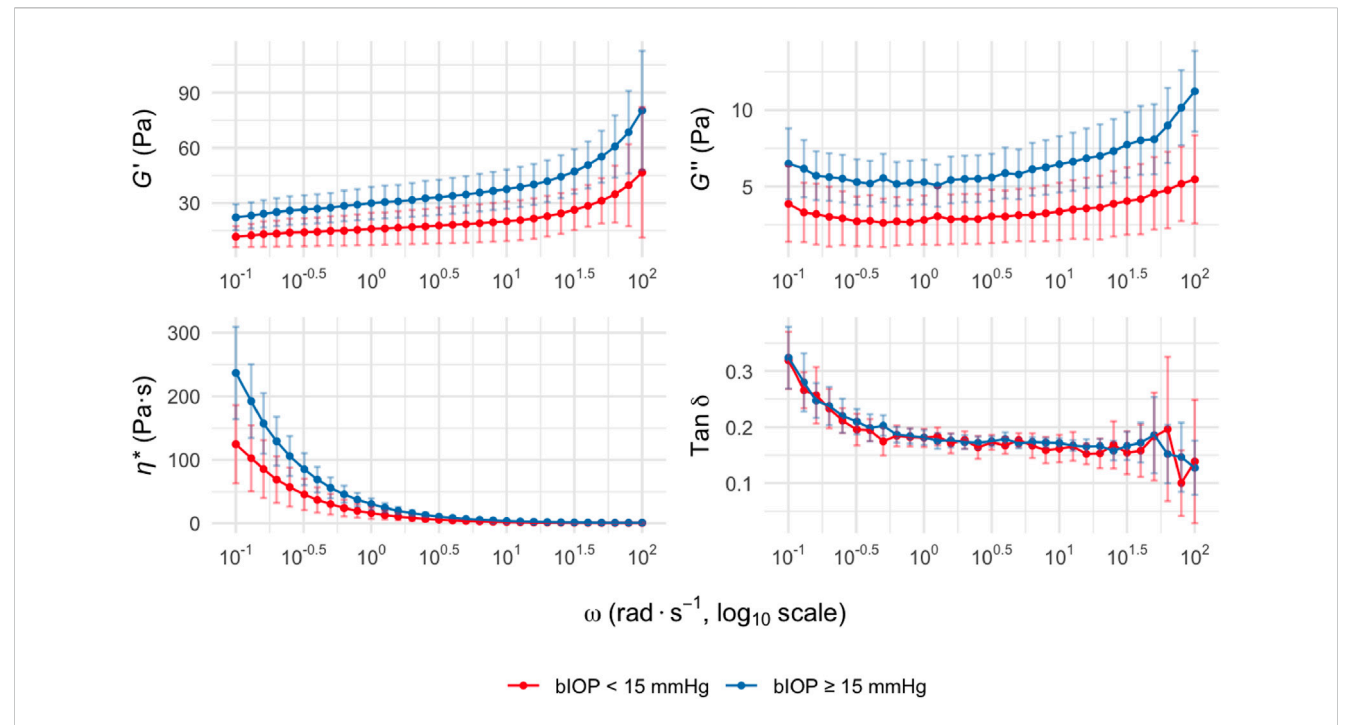
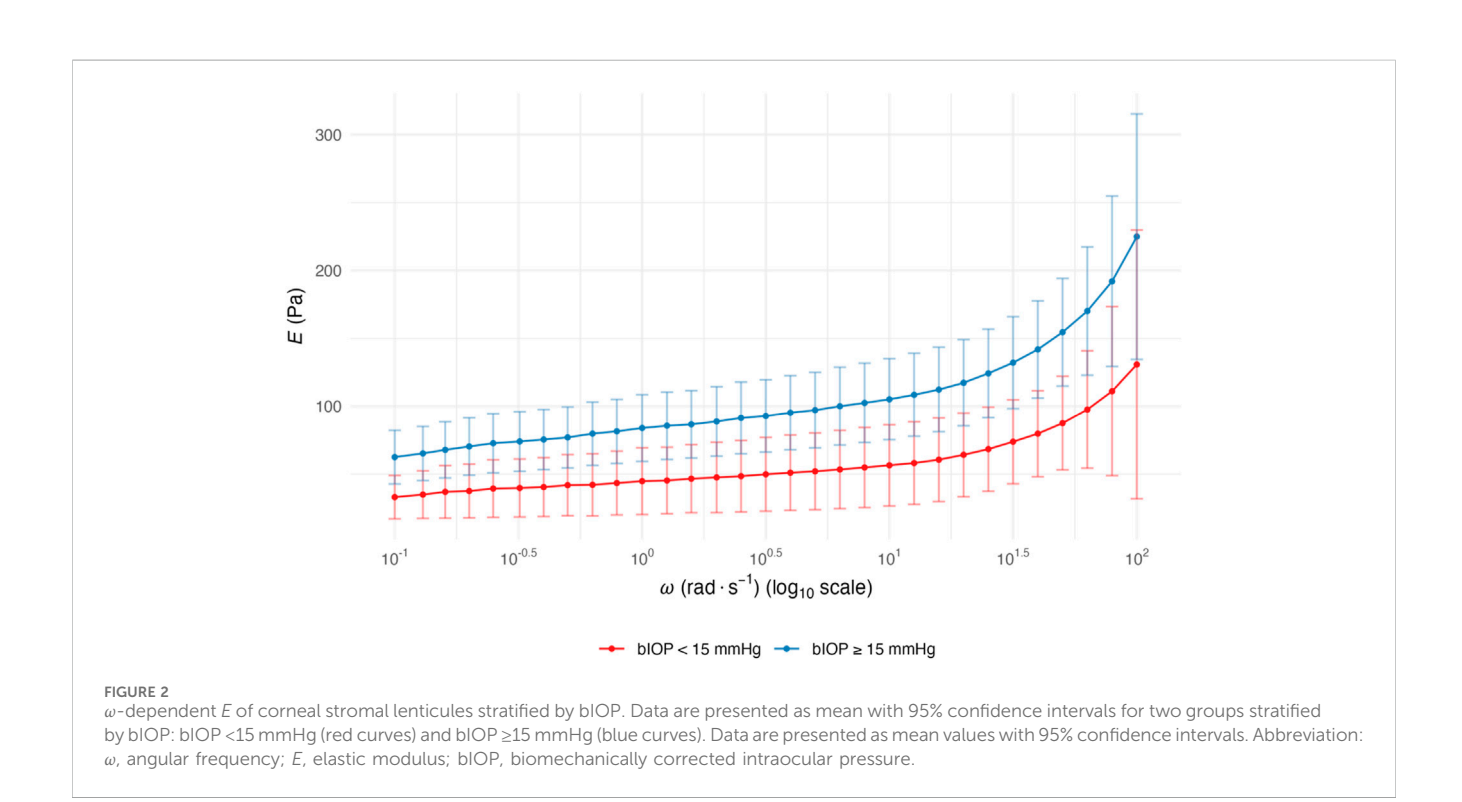


FIGURE 1
Viscoelastic parameters of corneal stromal lenticules at different oscillatory frequencies. G', G'', η^* , and $\tan \delta$ are plotted versus ω . Data are presented as mean with 95% confidence intervals for two groups stratified by bIOP: bIOP <15 mmHg (red curves) and bIOP \geq 15 mmHg (blue curves). Data are presented as mean values with 95% confidence intervals. Abbreviation: G', Storage modulus; G'', loss modulus; G'', complex viscosity; G'', loss tangent; G'', angular frequency; bIOP, biomechanically corrected intraocular pressure.



physiological conditions. Considered alongside our *ex vivo* modulus, the data suggest that within the physiological IOP range, higher baseline pressure elevates the cornea's stiffness "offset" while maintaining the ratio of stored to dissipated energy.

Distinguishing an overall stiffness shift from invariant δ may refine constitutive models and inform early risk stratification in pressure-related ocular disorders, including glaucoma and keratoconus.

Understanding how IOP, eye rubbing, and stromal mechanics interact is particularly important for translational relevance (Ben-Eli et al., 2019). Eye rubbing directly perturbs corneal optics and transiently elevates IOP; experimental application of "light" and "firm" digital forces to eyes with a baseline IOP of 15 mmHg can increase IOP by approximately twofold and fourfold, respectively (McMonnies and Boneham, 2007; McMonnies, 2008). Repetitive mechanical stimulation may also promote corneal thinning and reduce rigidity, potentially increasing the risk of ectasia such as keratoconus (Balasubramanian et al., 2013; Dou et al., 2022). In eyes with elevated bIOP, remodeling of the stromal matrix could further stiffen tissue and enhance resistance to torsional stress (Petroll et al., 2020). However, the torsional stresses and strains produced by vigorous eye rubbing may exceed the magnitudes tested here; future studies should examine whether corneas with different baseline bIOP exhibit differential resilience to acute IOP spikes and whether this modulates susceptibility to keratoconus onset or

The bIOP-stiffness association may inform refractive surgery planning. Lower baseline bIOP (reduced stiffness) could increase post-SMILE ectasia risk with aggressive ablation (Sinha Roy and Shetty, 2017), whereas higher bIOP may expand safety margins for high-myopia corrections. For lenticule transplantation (Ganesh et al., 2014), bIOP-matched donor-recipient pairing could optimize biomechanical integration. Pre-operative bIOP assessment may thus refine patient selection for precision refractive surgery.

This study has several limitations. Lenticules were sourced from a narrow age range of myopic SMILE patients, which may not extrapolate to pediatric or elderly populations with age-related collagen differences (Elsheikh et al., 2007; Whitford et al., 2015). Tissue hydration was controlled via BSS immersion at 37 °C, but ex vivo conditions may differ from in vivo endothelial regulation, and potential swelling artifacts could slightly overestimate compliance. The tested strain amplitude (1%) and frequency range (0.1-100 rad s⁻¹) interrogated the linear viscoelastic regime but may not capture strain-rate-dependent stiffening or nonlinear responses under rapid transient deformations (Whitford et al., 2018). An isotropic material assumption was applied despite documented stromal anisotropy (Meek and Knupp, 2015). Additionally, rheometry cannot resolve depth-dependent heterogeneity across stromal layers. Future work should integrate Brillouin optical microscopy for depth-resolved stiffness (Scarcelli et al., 2012), optical coherence elastography for strain visualization (Wang and Larin, 2015), second-harmonic generation for collagen architecture, and finite element modeling with patient-specific geometry and anisotropic constitutive laws to simulate pathological loading scenarios such as acute IOP spikes or postsurgical remodeling (Simonini and Pandolfi, 2015). This multiscale framework would enable translation of bIOP-modulus relationships into individualized risk prediction tools for keratoconus, glaucoma, or post-refractive ectasia.

In summary, strain-controlled torsional-shear rheometry reveals that higher physiological IOP is mirrored by a consistent upward shift in corneal stiffness, while the viscoelastic loss factor remains unaltered. This separation of a stiffness offset from invariant the viscoelastic loss factor offering a path to refine constitutive models and to develop biomechanical markers for early risk stratification in pressure-related ocular diseases.

Data availability statement

The raw data supporting the conclusions of this article will be made available by the authors, without undue reservation.

Ethics statement

The studies involving humans were approved by the Ethics Committee of Zhongshan Ophthalmic Center. The studies were conducted in accordance with the local legislation and institutional requirements. The participants provided their written informed consent to participate in this study.

Author contributions

XY: Data curation, Funding acquisition, Investigation, Writing – original draft, Writing – review and editing. QR: Conceptualization, Formal Analysis, Investigation, Methodology, Visualization, Writing – original draft, Writing – review and editing. XK: Validation, Writing – review and editing. PS: Validation, Writing – review and editing. CL: Data curation, Writing – review and editing. QL: Supervision, Writing – review and editing. PW: Project administration, Supervision, Writing – review and editing.

Funding

The author(s) declare that financial support was received for the research and/or publication of this article. Supported by the Science and Technology Innovation Projects of Foshan (grant no. 2420001003578).

Acknowledgements

The authors thank Jupeng Zhao and Limian Lin for their kind help.

Conflict of interest

The authors declare that the research was conducted in the absence of any commercial or financial relationships that could be construed as a potential conflict of interest.

Generative AI statement

The author(s) declare that no Generative AI was used in the creation of this manuscript.

Any alternative text (alt text) provided alongside figures in this article has been generated by Frontiers with the support of artificial intelligence and reasonable efforts have been made to ensure accuracy, including review by the authors wherever possible. If you identify any issues, please contact us.

Publisher's note

All claims expressed in this article are solely those of the authors and do not necessarily represent those of their affiliated organizations, or those of the publisher, the editors and the reviewers. Any product that may be evaluated in this article, or claim that may be made by its manufacturer, is not guaranteed or endorsed by the publisher.

References

Balasubramanian, S. A., Pye, D. C., and Willcox, M. D. (2013). Effects of eye rubbing on the levels of protease, protease activity and cytokines in tears: relevance in keratoconus. *Clin. Exp. Optom.* 96 (2), 214–218. doi:10.1111/cxo.12038

Ben-Eli, H., Erdinest, N., and Solomon, A. (2019). Pathogenesis and complications of chronic eye rubbing in ocular allergy. *Curr. Opin. Allergy Clin. Immunol.* 19 (5), 526–534. doi:10.1097/ACI.00000000000000571

Beylergil, S. B., Kilbane, C., Shaikh, A. G., and Ghasia, F. F. (2022). Eye movements in parkinson's disease during visual search. *J. Neurol. Sci.* 440, 120299. doi:10.1016/j.jns. 2022.120299

Dou, S., Wang, Q., Zhang, B., Wei, C., Wang, H., Liu, T., et al. (2022). Single-cell atlas of keratoconus corneas revealed aberrant transcriptional signatures and implicated mechanical stretch as a trigger for keratoconus pathogenesis. *Cell Discov.* 8 (1), 66. doi:10.1038/s41421-022-00397-z

Eliasy, A., Chen, K. J., Vinciguerra, R., Lopes, B. T., Abass, A., Vinciguerra, P., et al. (2019). Determination of corneal biomechanical behavior *in-vivo* for healthy eyes using CorVis ST tonometry: stress-strain index. *Front. Bioeng. Biotechnol.* 7, 105. doi:10.3389/fbioe.2019.00105

Elsheikh, A., Wang, D., Brown, M., Rama, P., Campanelli, M., and Pye, D. (2007). Assessment of corneal biomechanical properties and their variation with age. *Curr. Eye Res.* 32 (1), 11–19. doi:10.1080/02713680601077145

Ford, M. R., Dupps, W. J., Jr., Rollins, A. M., Sinha, R. A., and Hu, Z. (2011). Method for optical coherence elastography of the cornea. *J. Biomed. Opt.* 16 (1), 016005. doi:10. 1117/1.3526701

Ganesh, S., Brar, S., and Rao, P. A. (2014). Cryopreservation of extracted corneal lenticules after small incision lenticule extraction for potential use in human subjects. *Cornea* 33 (12), 1355–1362. doi:10.1097/ICO.000000000000276

Hatami-Marbini, H. (2014). Viscoelastic shear properties of the corneal stroma. J. Biomech. 47 (3), 723–728. doi:10.1016/j.jbiomech.2013.11.019

Kim, M., Kim, T. W., Weinreb, R. N., Lee, E. J., and Seo, J. H. (2014). Spontaneous retinal venous pulsation and disc hemorrhage in open-angle glaucoma. *Invest Ophthalmol. Vis. Sci.* 55 (5), 2822–2826. doi:10.1167/iovs.13-13836

Liu, M. X., Zhou, M., Li, D. L., Dong, X. X., Liang, G., and Pan, C. W. (2023). Corneal biomechanics in primary open angle glaucoma and ocular hypertension: a systematic review and meta-analysis. *J. Glaucoma* 32 (3), e24–e32. doi:10.1097/IJG. 0000000000002170

McMonnies, C. W. (2008). Management of chronic habits of abnormal eye rubbing. Cont. Lens Anterior Eye 31 (2), 95–102. doi:10.1016/j.clae.2007.07.008

McMonnies, C. W., and Boneham, G. C. (2007). Corneal curvature stability with increased intraocular pressure. *Eye Contact Lens* 33 (3), 130–137. doi:10.1097/01.icl. 0000246910.02437.62

Meek, K. M., and Knupp, C. (2015). Corneal structure and transparency. *Prog. Retin Eye Res.* 49, 1–16. doi:10.1016/j.preteyeres.2015.07.001

Meek, K. M., Knupp, C., Lewis, P. N., Morgan, S. R., and Hayes, S. (2025). Structural control of corneal transparency, refractive power and dynamics. *Eye (Lond)* 39 (4), 644–650. doi:10.1038/s41433-024-02969-7

Miao, Y. Y., Ma, X. M., Qu, Z. X., Eliasy, A., Wu, B. W., Xu, H., et al. (2024). Performance of Corvis ST parameters including updated stress-strain index in differentiating between normal, Forme-Fruste, subclinical, and clinical keratoconic eyes. *Am. J. Ophthalmol.* 258, 196–207. doi:10.1016/j.ajo.2023.10.015

Pang, J. J. (2021). Roles of the ocular pressure, pressure-sensitive ion channel, and elasticity in pressure-induced retinal diseases. *Neural Regen. Res.* 16 (1), 68–72. doi:10. 4103/1673-5374.286953

Petroll, W. M., Varner, V. D., and Schmidtke, D. W. (2020). Keratocyte mechanobiology. Exp. Eye Res. 200, 108228. doi:10.1016/j.exer.2020.108228

Pillunat, K. R., Herber, R., Spoerl, E., Erb, C., and Pillunat, L. E. (2019). A new biomechanical glaucoma factor to discriminate normal eyes from normal pressure glaucoma eyes. *Acta Ophthalmol.* 97 (7), e962–e967. doi:10.1111/aos.14115

Renato, J., Ramos, I., Luz, A., Faria, F. C., Steinmueller, A., Krug, M., et al. (2013). Avaliação Dinâmica com fotografia de Scheimpflug de alta velocidade para avaliar as propriedades biomecânicas da córnea. 72(2), 99–102. doi:10.1590/s0034-72802013000200005

Roberts, C. J. (2014). Concepts and misconceptions in corneal biomechanics. J. Cataract. Refract Surg. 40 (6), 862–869. doi:10.1016/j.jcrs.2014.04.019

Roberts, C. J., Mahmoud, A. M., Bons, J. P., Hossain, A., Elsheikh, A., Vinciguerra, R., et al. (2017). Introduction of two novel stiffness parameters and interpretation of air puff-induced biomechanical deformation parameters with a dynamic scheimpflug analyzer. *J. Refract Surg.* 33 (4), 266–273. doi:10.3928/1081597X-20161221-03

Scarcelli, G., Pineda, R., and Yun, S. H. (2012). Brillouin optical microscopy for corneal biomechanics. *Invest Ophthalmol. Vis. Sci.* 53 (1), 185–190. doi:10.1167/iovs.11-8281

Simonini, I., and Pandolfi, A. (2015). Customized finite element modelling of the human cornea. *PLoS One* 10 (6), e0130426. doi:10.1371/journal.pone.0130426

Sinha Roy, A., and Shetty, R. (2017). Ectasia after SMILE: correct interpretation of biomechanical Hypothesis. *J. Refract Surg.* 33 (1), 66. doi:10.3928/1081597X-20161018-03

Vinciguerra, R., Ambrosio, R., Jr., Elsheikh, A., Roberts, C. J., Lopes, B., Morenghi, E., et al. (2016). Detection of keratoconus with a new biomechanical index. *J. Refract Surg.* 32 (12), 803–810. doi:10.3928/1081597X-20160629-01

Vinciguerra, R., Rehman, S., Vallabh, N. A., Batterbury, M., Czanner, G., Choudhary, A., et al. (2020). Corneal biomechanics and biomechanically corrected intraocular pressure in primary open-angle glaucoma, ocular hypertension and controls. *Br. J. Ophthalmol.* 104 (1), 121–126. doi:10.1136/bjophthalmol-2018-313493

Vinciguerra, R., Ambrosio, R., Jr., Elsheikh, A., Hafezi, F., Yong Kang, D. S., Kermani, O., et al. (2021). Detection of postlaser vision correction ectasia with a new combined biomechanical index. *J. Cataract. Refract Surg.* 47 (10), 1314–1318. doi:10.1097/j.jcrs. 0000000000000629

Wang, S., and Larin, K. V. (2015). Optical coherence elastography for tissue characterization: a review. $J.\ Biophot.\ 8$ (4), 279–302. doi:10.1002/jbio.201400108

Wei, Y., Cai, Y., Bao, C., Zhu, Y., and Pan, Y. (2023). The role of corneal biomechanics in visual field progression of primary open-angle glaucoma with ocular normotension or hypertension: a prospective longitude study. *Front. Bioeng. Biotechnol.* 11, 1174419. doi:10.3389/fbioe.2023.1174419

Whitford, C., Studer, H., Boote, C., Meek, K. M., and Elsheikh, A. (2015). Biomechanical model of the human cornea: considering shear stiffness and regional variation of collagen anisotropy and density. *J. Mech. Behav. Biomed. Mater* 42, 76–87. doi:10.1016/j.jmbbm.2014.11.006

Whitford, C., Movchan, N. V., Studer, H., and Elsheikh, A. (2018). A viscoelastic anisotropic hyperelastic constitutive model of the human cornea. *Biomech. Model Mechanobiol.* 17 (1), 19–29. doi:10.1007/s10237-017-0942-2

Xu, Z., Hysi, P., and Khawaja, A. P. (2021). Genetic determinants of intraocular pressure. *Annu. Rev. Vis. Sci.* 7, 727–746. doi:10.1146/annurev-vision-031021-095225

Zhang, H., Eliasy, A., Lopes, B., Abass, A., Vinciguerra, R., Vinciguerra, P., et al. (2021). Stress-Strain Index map: a new way to represent corneal material stiffness. *Front. Bioeng. Biotechnol.* 9, 640434. doi:10.3389/fbioe.2021.640434